Microfluidics and Nanofluidics (2018) 22:97
https://doi.org/10.1007/s10404-018-2118-5

RESEARCH PAPER

Soft lithography based on photolithography and two-photon polymerization

Yang Lin[1] · Can Gao[1] · Dmitry Gritsenko[1] · Ran Zhou[2] · Jie Xu[1]

Received: 13 April 2018 / Accepted: 16 August 2018 / Published online: 23 August 2018

Abstract

Over the past decades, soft lithography has greatly facilitated the development of microfluidics due to its simplicity and cost-effectiveness. Besides, numerous fabrication techniques such as multi-layer photolithography, stereolithography and other methods have been developed to fabricate moulds with complex 3D structures nowadays. But these methods are usually not beneficial for microfluidic applications either because of low resolution or sophisticated fabrication procedures. Besides, high-resolution methods such as two-photon lithography, electron-beam lithography, and focused ion beam are often restricted by fabrication speed and total fabricated volume. Nonetheless, the region of interest in typical microfluidic devices is usually very small while the rest of the structure does not require complex 3D fabrication methods. Herein, conventional photolithography and two-photon polymerization are combined for the first time to form a simple hybrid approach in fabricating master moulds for soft lithography. It not only benefits from convenience of photolithography, but also gives rise to complex 3D structures with high resolution based on two-photon polymerization. In this paper, various tests have been conducted to further study its performance, and a passive micromixer has been created as a demonstration for microfluidic applications.

Keywords Soft lithography · Photolithography · Two-photon polymerization · Master mould · SU-8

1 Introduction

Soft lithography has become an important technique in microelectromechanical systems (MEMS) and micro total analysis systems (μTAS, or lab on a chip) nowadays (Rogers and Nuzzo 2005), as evidenced by numerous examples in micro- and nano-fabrication (Qin et al. 2010), electronics (Jeon et al. 1998), chemistry (Pang et al. 2003), biology (Kane et al. 2006), pharmaceutics (Whitesides et al. 2001), and microfluidics (Kim et al. 2008). Compared to other microfabrication techniques (e.g., photolithography and electron-beam lithography), soft lithography possesses several unique advantages (Xia and Whitesides 1998). For instance, it is more cost-effective and requires neither too much expertise nor sophisticated equipment (Folch 2016). It is suitable for not only planar, but also non-planar surfaces; hence the structures with different heights are no longer obstacles (Kane et al. 2006). Besides, soft-lithography also provides a very good resolution (~ 35 nm), which is competitive even when compared with electron-beam lithography (~ 15 nm) (Waldner 2013; Xia and Whitesides 1998).

At present, several techniques that are classified as soft lithography have been developed, including microcontact printing (μCP) (Filipponi et al. 2016), replica molding (REM) (Carugo et al. 2016), microtransfer molding (Yang et al. 2000), solvent-assisted micromolding (King et al. 1997), micromolding in capillary (Kim et al. 1995), decal transfer lithography (Childs and Nuzzo 2002), nanoskiving (Xu et al. 2008), and so on. Among them, REM has been widely used in microfluidics, with elastomer polydimethylsiloxane (PDMS) as the key component to imprint patterned relief structures on the surfaces of master moulds (Folch 2016). Specifically, microstructures are first fabricated on substrates, then the mixture of PDMS precursors is poured onto the substrate, followed by baking using a hotplate or an

Electronic supplementary material The online version of this article (https://doi.org/10.1007/s10404-018-2118-5) contains supplementary material, which is available to authorized users.

✉ Yang Lin
ylin212@uic.edu

[1] Mechanical and Industrial Engineering, University of Illinois at Chicago, Chicago, IL 60607, USA

[2] Department of Mechanical and Civil Engineering, Purdue University Northwest, Hammond, IN 46323, USA

oven to induce cross-linking of the monomers. As the contact between PDMS precursors and the moulds is conformal, the reversed pattern of the microstructures from substrates is imprinted on PDMS after separation. Finally, the replica can be bonded to another substrate (e.g., glass slide) to create enclosed microchannels for further applications (Shin et al. 2003).

It is worth mentioning that PDMS possesses many superior advantages, which are quite attractive for microfluidic applications. To name a few, it has a great optical transparency (Schneider et al. 2009), gas permeability (Merkel et al. 2000), biocompatibility (Borenstein et al. 2010), and chemical inertness (Zhu et al. 2017). Hence, it has been widely used in biomedicine-related microfluidics over the past decades. Additionally, PDMS is soft and elastic, hereby it is also an ideal candidate for microscale valves and actuators (Choi et al. 2010). Although intrinsic hydrophobicity may be unfavourable for the introduction of aqueous solutions into channels, this shortcoming can be addressed via oxygen plasma (Tan et al. 2010). Last but not least, PDMS-based devices are relatively cheaper than the counterparts made via glass or silicon because of the ease of fabrication and multiple castings of a master mould.

However, as PDMS only imprints the structures on a master mould, leading the fabrication of master moulds the most pivotal step in soft lithography. To date, numerous mould-creating techniques have been developed, including photolithography (Huh et al. 2010), wet etching (Filipponi et al. 2016), reactive ion etching (Brittman et al. 2017), micromachining (Park et al. 2010), multiphoton lithography (Saive et al. 2017), stereolithography (Hwang et al. 2015), electron-beam lithography (Huang et al. 2004), focused ion beam (Li et al. 2003), and so forth. Among these techniques, photolithography is still the mainstream method for soft lithography due to its simplicity and high resolution. In a typical microfluidic application, negative-tone photoresist SU-8 is the most commonly used photoresist for photolithography due to its good chemical, mechanical properties as well as the capability of creating structures with high aspect ratio (over 25) (del Campo and Greiner 2007; Mata et al. 2006). Nevertheless, conventional photolithography is not impeccable. Creating three-dimensional (3D) structures are still challenging for photolithography. Although stacking multiple layers is able to compensate this drawback, the entire process becomes tedious and allows very little tolerance to operational errors during alignments (Mata et al. 2006). Besides, this approach only works for simple 3D designs, in which the curved structures are not included. To circumvent this issue, other techniques (e.g., 3D printing, electron-beam lithography) have been explored for soft lithography. For instance, 3D printed mould has been applied to fabricate PDMS-based microfluidic device on studies of cell stimulation recently (Kamei et al. 2015). In contrast to photolithography, this method does not require a clean room, and it enables the fabrication of real 3D structures. However, the created master moulds usually possess low resolution and high roughness (Kamei et al. 2015), which inhibit further applications, especially when small features are required. Fortunately, this downside can be solved using other mould-creating techniques such as electron-beam lithography, focused ion beam and so on. They possess the capabilities to fabricate complex 3D structures with high resolution. Furthermore, techniques such as deep ultraviolet (DUV) and extreme ultraviolet (EUV) can even achieve resolution as high as several tens of nanometres.

However, most of these advanced fabrication methods require vacuum conditions, herein their procedures and maintenance are usually time-consuming. Recently, two-photon polymerization (TPP), a promising stereolithography technique that does not require vacuum pumping, have also been investigated for soft lithography (Bernardeschi et al. 2016). In contrast to conventional stereolithography, two photons are absorbed simultaneously in TPP process instead of single photon. Owing to nonlinear absorption, this technique confines the volume (i.e., voxel) of photopolymerization at nanoscale; therefore, extremely high resolution can be obtained (Lin and Xu 2018). Besides, similar to typical additive manufacturing techniques, TPP directly creates final structures from digital CAD models, resulting in significantly less operation errors compared to other high-resolution techniques mentioned above. Finally, the implementation of laser with long wavelength brings several advantages such as lower absorption scattering, giving rise to a deeper penetration of light into materials; hence microstructures can be directly created inside photoresists.

On the contrary, it is also due to its high resolution structures are fabricated voxel by voxel in TPP process. Therefore, the fabrication time can be extremely long when it comes to the fabrication of large objects. For instance, writing a solid cubic structure of 50 μm × 50 μm × 10 μm can take up to around 3.5 h (Weiss and Marom 2015). At present, various methods have been explored and developed to speed up the process. To name a few, instead of writing a complete structure, Weiss and co-workers only wrote the internal skeletal supports as well as the outer shell. Unpolymerized photosensitive materials were encapsulated inside these backbones (Weiss and Marom 2015). Next, an extra UV exposure was used to induce a complete polymerization for the whole structure. As a result, the whole writing time has been reduced to 0.5 h. Similarly, Kurihara and colleagues first printed the frame structure using TPP and then filled the gaps with parylene (Kurihara et al. 2012). However, these treatments are still insufficient to make TPP an efficient method for creating master mould for soft lithography due to their complexity.

It is worth mentioning that in a typical microfluidic device, only small regions would require features with high resolution to achieve different purposes such as mixing, filtration and separation, while the remaining parts are mainly used to transport fluids and reagents. Herein, we present an innovative method to fabricate master moulds, which combines the ease of photolithography and high resolution of TPP. Photolithography is used to fabricate the majority of the mould, while TPP is applied only for small regions where high resolution is required. Generally speaking, these two methods can be proceeded separately. First, the main structure is created using SU-8 via photolithography, then the small region is filled by printing structures via TPP using SU-8 or other photosensitive materials. However, when it comes to the connection between the printed parts with existing structures, an overlapping area between two parts is inevitable. That is, the edges of solid SU-8 structures may receive a significantly excessive energy, and result in deformations during the printing process. Additionally, the refractive indices of solid and liquid SU-8 are different, thus deflections may occur during printing. Last, the separation of two steps also increases the time cost. Given these concerns, we perform the TPP process directly in the SU-8 film right after UV exposure of photolithography. Hereby, the same procedures (e.g., softbake and postbake) are applied to both structures exposed using different lights, and problems described above can be avoided.

2 Materials and methods

2.1 Fabrication of hybrid moulds

A thin glass cover slide (CS-30R15, Warner Instruments, CT) was used as a substrate to create master mould using hybrid method. Although silicon wafers possess several advantages (e.g., good thermal conductivity) compared to the glass slides for photolithography, it is not favourable for the hybrid fabrication process developed in this work. Owing to unwanted opaqueness, the structures fabricated via photolithography can hardly be found under the microscope during TPP process, not to mention the alignment between TPP-fabricated structures with existing ones. Therefore, the glass slides were chosen as substrates to fabricate master moulds. As shown in Fig. 1, the fabrication process can be divided into following steps:

1. Preparation of glass substrate.
   A glass cover slide was first cleaned thoroughly with acetone, methanol, and isopropyl alcohol consecutively. An extra oxygen plasma cleaning (PDC-001, Harrick Scientific Inc.) was also performed to further remove remaining organic residues. Afterwards, the glass slide was transferred to a hotplate (HS61, Torrey Pines Scientific) for 2 h at 180 °C, assuring better photoresist adhesion after the top surface of the glass slide was completely dehydrated (Kai 2004).
2. Spin coating of SU-8.
   After dehydration, the glass slide was transferred to a spin coater (Spin Coater, P6700, Specialty Coating Systems Inc.) immediately. SU-8 (SU-8 2025, MicroChem Corporation, MA) was then dispensed using a

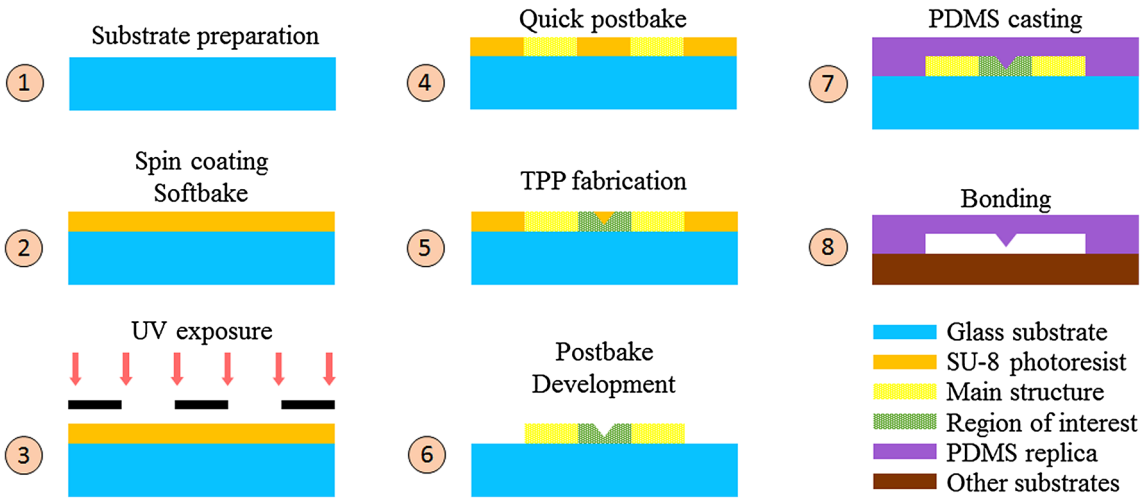

Fig. 1 Schematic illustration for hybrid fabrication process based on photolithography and two-photon polymerization

disposable plastic syringe (10 ml BD syringe), covering two-thirds of the area of glass slide. The spinning speed was then controlled according to the data sheet of SU-8. In our case, 2000 rpm was used to form a photoresist film with thickness of 40 μm. In addition, the edge beads should be removed for an intimate contact between the glass slide and photomask during UV exposure (Miyajima and Mehregany 1995).

3. Softbake and exposure of SU-8 film.

   It is worth noting that glass has a smaller thermal conductivity compared to silicon wafer; therefore, a longer softbake time is required. Herein, the time used to heat up the glass slide (~30 s) should be added to the total time. After the sample cooled down to the room temperature, a clear photomask (FineLine Imaging Inc., CO) with segmented pattern was attached to 5 × 5 clear glass (Front Range PhotoMask, CO) and then loaded in a mask aligner (MA6/BA6, Karl-Süss, Germany). A long bandpass filtre (Omega Optical Inc., VT) was also applied to reduce the exposure from UV radiation with wavelength below 350 nm, which may cause non-vertical wall formation. In addition, the exposure time should be elongated when taking glass substrates and optical filtre into account.

4. TPP fabrication.

   As a cationic-type photoresist, SU-8 allows the cross-linking of oligomeric epoxides only after receiving sufficient heat during the postbake (Baldacchini 2015; Sun et al. 2005). Thereby, a quick postbake is indispensable to visualize the exposed pattern for the alignment. To put it simply, the sample was transferred to the hotplate with the temperature at 95 °C again. In about 20 s, the pattern emerged. When the sample was cooled down to the room temperature, it was attached to the holder of TPP system (Nanoscribe GmbH, Germany) using tape, followed by adding immersion oil (518 F Zeiss, Carl Zeiss, NY) on the surfaces (Fig. 2a). The introduction of immersion oil promoted the seeking of interfaces between the substrates and SU-8 films. Additionally, as for the hybrid fabrication method, one should always care about the accuracy of connection between one and the other. Hence, the alignment of printing structures with existing patterns was of the utmost importance (Supplementary material). Moreover, the intensity of laser power used in TPP was another crucial factor to be controlled during the fabrication process. A high-intensity laser usually leads to bubbling in the film, thus hindering the fabrication. This phenomenon can be attributed to a remarkable temperature increase in overexposed regions (Jiang et al. 2014), hence the photoresist may be boiled and generate bubbles. On the other hand, a low-intensity laser gives rise to insufficient cross-linking, thereby the structures maybe deformed during development.

5. Postbake and development.

   After the printing process finished, the sample was transferred to the hotplate for postbake. Propylene glycol methyl ether acetate (PGMEA, MicroChem Corporation, MA) developer was used to wash unpolymerized SU-8 from the glass after cooling the sample down to the room temperature.

2.2 PDMS casting and bonding

To prepare PDMS replica using the mould prepared as described above, PDMS mixture (Sylgard 184, Dow Corning, MI) with 10:1 base to curing agent mixing ratio was first stirred vigorously, and then degassed thoroughly using a vacuum desiccator (Bel-Art Scienceware, NJ). Afterwards, the mixture was gently poured onto the master mould, followed by degassing again. It is worth noting that the glass substrates were very thin, thus they can be easily broken when peeling the PDMS off. Hereby, we fixed them in a bigger container such as a Petri dish with the tape (Supplementary material). The container was then transferred to

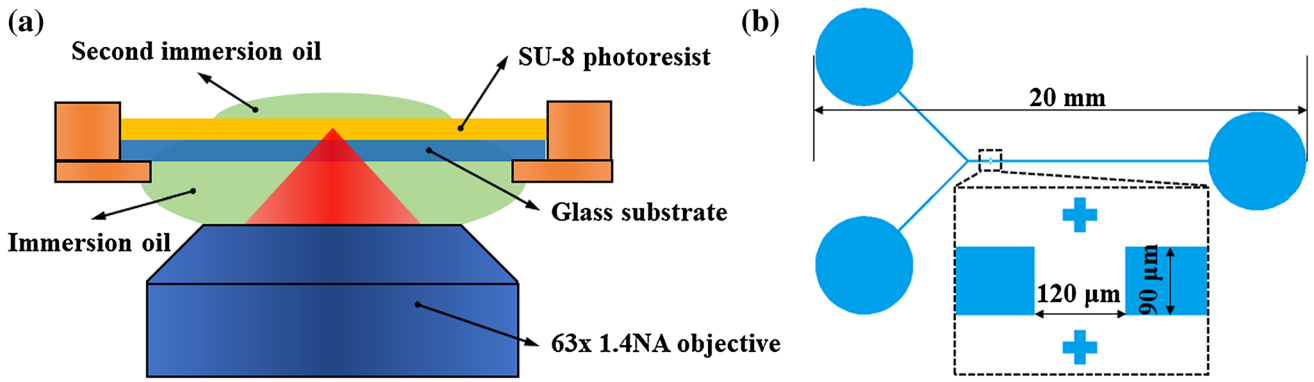

Fig. 2 **a** Schematic illustration of the configuration for TPP process in hybrid method. **b** Scheme of a common mixing channel with a rectangular gap in the main channel

an oven for 2 h at 65 °C, and PDMS replica was peeled off gently. The replica was then bonded to other substrates such as glass slides.

3 Results and discussion

To better understand the performance and limitations of this hybrid fabrication method, we have examined several parameters and key steps that may affect the results using a common mixing channel with a rectangular gap (120 µm in length and 90 µm in width) in the main channel (Fig. 2b). In addition, various designs have been adopted to show its capabilities in fabricating master moulds with 3D geometries in the region of interest. Last, a simple passive micromixer was fabricated and used to demonstrate its applications in microfluidics.

3.1 Influence of adding immersion oil

To print 3D structures in the region of interest, one of the key problems to tackle is the seeking of correct interface between the substrates and the photosensitive materials. Otherwise, the laser may start printing inside the glass, resulting in incomplete structures, or the entire structure may float inside photoresist and be washed away after the development. Besides, the interface seeking is usually based on the difference of refractive indices of substrates and photoresists in TPP system. Hereby, adding immersion oil (that has refractive index identical to glass) between the objective lens and the glass promotes the seeking of interfaces, since it eliminates the interface between substrates and air. But on the other hand, we found that if the immersion oil was only added to the bottom side of the glass, the exposed pattern was difficult to find under the microscope (Fig. 3a). Even though the pattern has emerged if the focal point was manually moved away from the substrate, the pattern shown under microscope was shifted to another position as well. Another approach to find a clear exposed pattern was adding one more droplet of immersion oil on the top of the SU-8 film. In this case, the pattern was clear as shown in Fig. 3b, and the immersion oil on both sides of the sample can be washed away during development. The enhancement of the microscope viewing may be ascribed to the backreflection from the second drop of immersion oil, which also affected the laser intensity required for polymerization. We found that laser with lower intensity may induce bubble formation with addition of second drop. Herein, lower laser intensity should be used and it satisfied the requirement of polymerization. This configuration also exerted additional stress on the final structures during development due to the adhesion of immersion oil to the SU-8 photoresist especially when the oil became drier after postbake. Nevertheless, given the fact that a better view of exposed pattern is of the utmost importance for a hybrid method, we have adopted this method for all further tests.

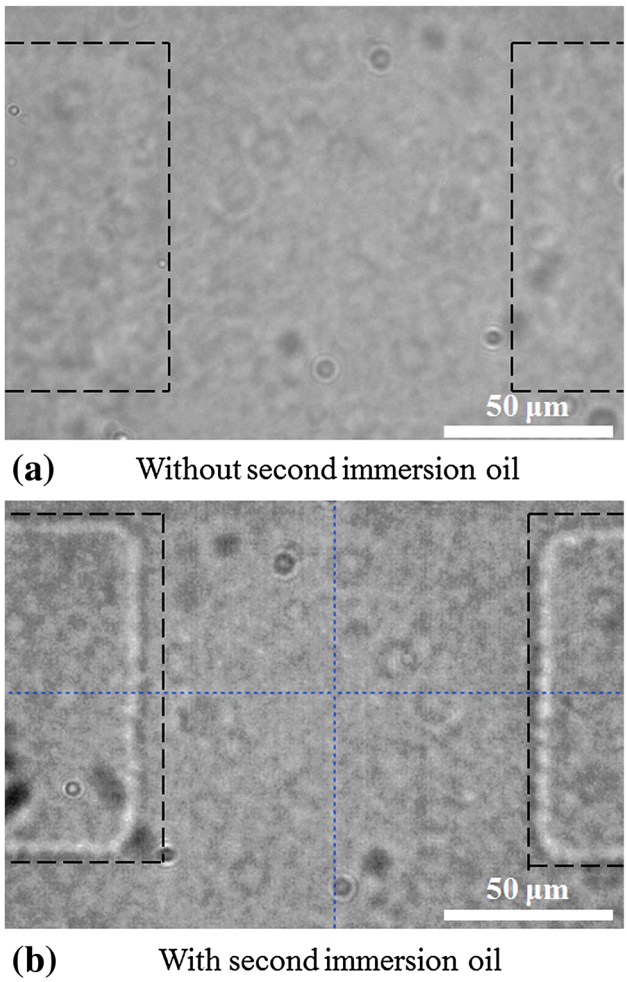

Fig. 3 Influence of adding second droplet of immersion oil. **a** The immersion oil was only added on the bottom side of the substrate. The exposed pattern was hard to find. **b** The immersion oil was added on both sides of the substrate. A clear edge of exposed pattern can be found under microscope

3.2 Influence of quick postbaking time

In contrast to conventional photolithography, our method requires another quick postbake to visualize the exposed pattern. Generally speaking, a longer postbaking time results in better cross-linking of oligomeric epoxides in SU-8. However, it not only increases the time cost, but also makes the SU-8 film more difficult to develop (Narimannezhad et al. 2013). Therefore, we have examined the optimal quick postbaking time to achieve a clear view of exposed pattern. As the exposed pattern became visible after putting the sample on the hotplate at 95 °C for 10 s, we have chosen four different samples with different quick postbaking times of 10, 20,

30, 40 s, respectively. As shown in Fig. 4, the exposed pattern in sample A that has undergone 10 s of quick postbake was difficult to find, not to mention the alignment. On the contrary, sample B has received more heat (20 s) and its pattern was much clearer under the microscope. However, if the time of quick postbake was further increased, the patterns became a little bit blur again. Herein, we have chosen 20 s as an optimal quick postbaking time in the following tests.

3.3 Selection of laser intensity

As described above, a high-intensity laser usually induces bubble formation during TPP process while the low-intensity laser results in insufficient cross-linking. Besides, the optimal laser intensity also depends on the properties of the photosensitive materials. Therefore, we have done a series of tests on fabrication of a truss structure using different power intensities (15 mW, 17.5 mW, 20 mW, 22.5 mW, and 25 mW). We found it was quite challenging to fabricate truss using 15 mW as the structures were too soft and washed away after development. Moreover, weak power intensities (17.5 and 20 mW) have given rise to undesired deformation of the final structures (Fig. 5). This was attributed to insufficient cross-linking, making the structures vulnerable, and hence some parts of the trusses were washed away. On the contrary, the higher intensity (22.5 mW) resulted in a firm structure that matched the CAD model. However, if the power intensity was too strong (e.g., 25 mW), the bubbling maybe induced and demolished the structures. Nevertheless, it is worth mentioning that the optimal intensity is flexible, as it depends on the structure properties and geometries. When the cross-section of the structures is large enough, the favourable power intensity should be smaller. This can be attributed to the overlapping exposures between the adjacent voxels.

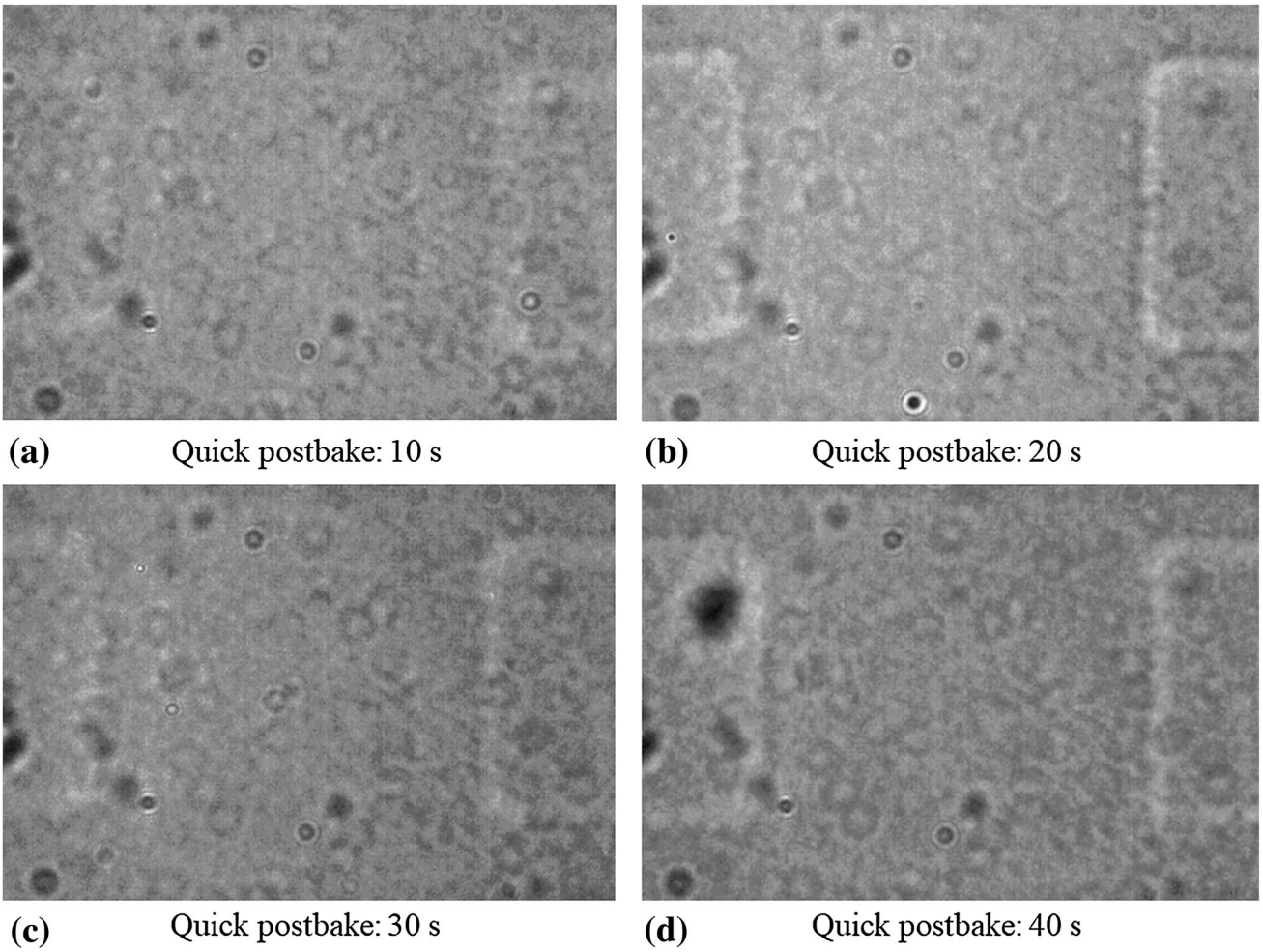

Fig. 4 Study of the impact of quick postbaking time on finding exposed pattern. A quick postbake of 20 s showed the clearest edges of exposed pattern

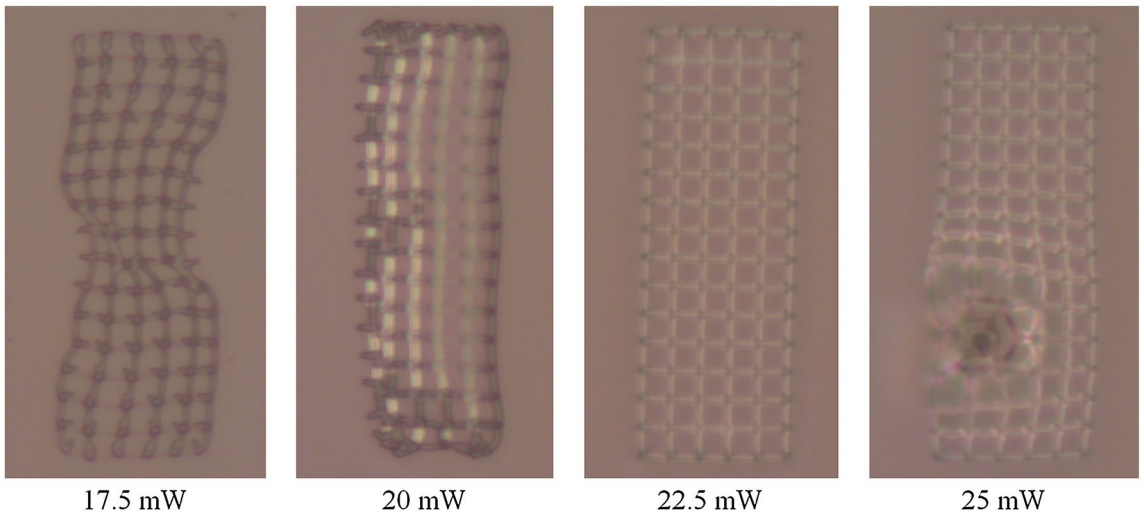

Fig. 5 Low-intensity laser led to undesired deformation of the final truss structures while a high-intensity laser may induce bubble formation during TPP process. Therefore, a careful calibration of laser intensity is highly recommended before the fabrication

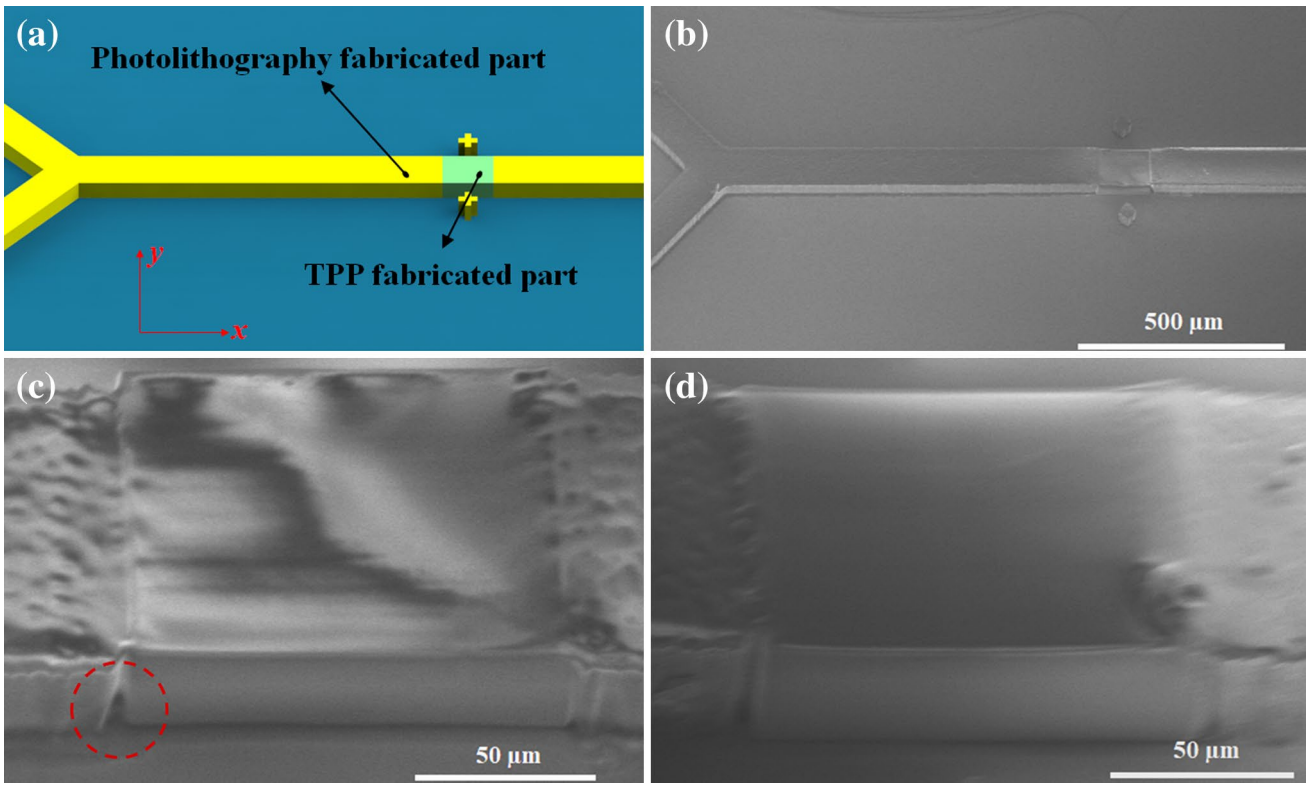

Fig. 6 A simple block was used to test the feasiblity of the proposed method. **a** A 3D design that manifests the idea of how the block is used to connect segmented parts. **b** SEM image of the hybrid structure fabricated by photolithography and TPP. **c** Zoomed SEM images of the regions where the structures connected with the block for the gap of identical dimensions. A small opening between two structures was marked with red circle. **d** Elongated block used to compensate the gap between two structures

3.4 Proof-of-the-concept fabrication

The first design used to demonstrate the capability of combining photolithography and TPP is a simple block that connects two segmented microchannels (Fig. 6a). Even though the desired thickness of SU-8 film (40 μm as a demonstration) on the glass is predictable according to protocol, it is impossible to know the exact value before the development. Given that there is no SU-8 above the top surface of the photoresist film, TPP process only happens in the immersion oil for the part extruded. Therefore, thick designs that exceed photoresist film should result in identical structures with the same thickness. However, the proper estimation of the final height is still demanding to reduce the fabrication time wasted on the extruded parts. Based on this assumption, we printed a block with the same length and width, but of the larger height (45 μm).

To give a closer look on the final structure, scanning electron microscopy (SEM) system (Hitachi S-3000N-VP-SEM, Japan) was used. As showed in Fig. 6b, a simple block fabricated by TPP was successfully connected to the segmented microchannel fabricated using photolithography. Nevertheless, after zooming in, the surface of the final structure was not as smooth as expected (Fig. 6c). This thickness variation could arise from the flowing of SU-8 during softbake (Lin et al. 2002). Furthermore, a contact profiler (P7, KLA-Tencor, CA) was used to measure the surface profile in the region where hybrid structures were connected. It was found that the roughness of the surface fabricated by photolithography was around 0.2 μm, which was acceptable for the majority of microfluidic applications. Additionally, there were two small ridges (less than 1.5 μm in height) in the connecting areas. This problem may be attributed to different shrinkage rates between the photolithography-fabricated parts and TPP-fabricated parts. Nevertheless, compared to the entire thickness of 40 μm, the difference was almost negligible. A small opening was also found in the bottom of the connecting region, which was probably due to low resolution and transmittance from plastic mask, and can be simply improved if high-resolution masks are used. Alternatively, an elongated structure (e.g., length of 130 μm) with the large overlaps can be adopted to compensate the deficiency (Fig. 6d). Last but not least, a small deviation was also found in x direction, and it was an inevitable shortcoming for the proposed hybrid method as the alignment of the printed structure and exposed pattern depended on the clarity of edges in the exposed pattern.

3.5 Various microstructures fabricated using hybrid methods

To further investigate the performance of hybrid method, several microstructures with different designs have been fabricated. As presented in Fig. 7a, a series of grooves having the same height of 5 μm, but different widths ranging from 0.5 to 5.0 μm with an increment of 0.5 μm were fabricated. Specifically, the grooves with the widths more than 1.5 μm were successfully fabricated with the vertical walls as expected. However, two grooves with the widths of 0.5 and 1.0 μm collapsed and the walls between them were connected to each other, which can be attributed to their high aspect ratios. Nonetheless, the results have proven this method to be promising in fabrication of 3D master moulds with high resolution. Additionally, other designs in a connecting block were also fabricated (Fig. 7b, c, d), including cone-shaped cavities, cylindrical pillars, and UIC characters, respectively. Their PDMS replicas are shown in Fig. 7e, f, g, respectively.

In addition, owing to the rapid photolithography process, the time costs for these hybrid structures were much less than that of the structures printed solely by TPP (Table 1). For instance, for a micromixer mould with a connecting block that has structure of cylindrical pillars, the pure TPP for the main channel via solid TPP printing (i.e., solidification at each point with 63x NA 1.4 objective) required 928 h and 20 min, which was almost impossible to achieve. Although adopting scaffold method (i.e., solidification only existed on external surfaces and internal scaffolds) or using other objective (e.g., 25x objective) can mitigate the workload, the final time cost was still huge, not to mention low resolution obtained from 25x objective. Besides, when printing large structure using TPP, stitching has to be applied because of the limitation of the printing field. Herein, the final structures were made of numerous small parts, which gave rise to non-smooth surfaces or even steps between them. On the other hand, the connection in the proposed hybrid method is only required between the regions of interest and the main channels, hence the steps only exist in limited areas.

3.6 Demonstration of microfluidic application: a passive micromixer

As aforementioned, soft lithography has become a commonly used method in microfluidics, and the proposed fabrication method has opened a new door to fabricate reliable master moulds for soft lithography. Micromixer is an important component that has been commonly used in microfluidics due to the fact that viscous force becomes ineligible at microscale and the laminar flow is dominant in the most cases. Hence, mixing in a microchannel is mainly fulfilled by means of passive diffusion, being insufficient for most scenarios. Nowadays, various micromixers have been developed to facilitate mixing at microscale, including passive and active micromixers. In this paper, we have created a passive micromixer to demonstrate the capability of hybrid fabrication method for microfluidic applications. Specifically, the

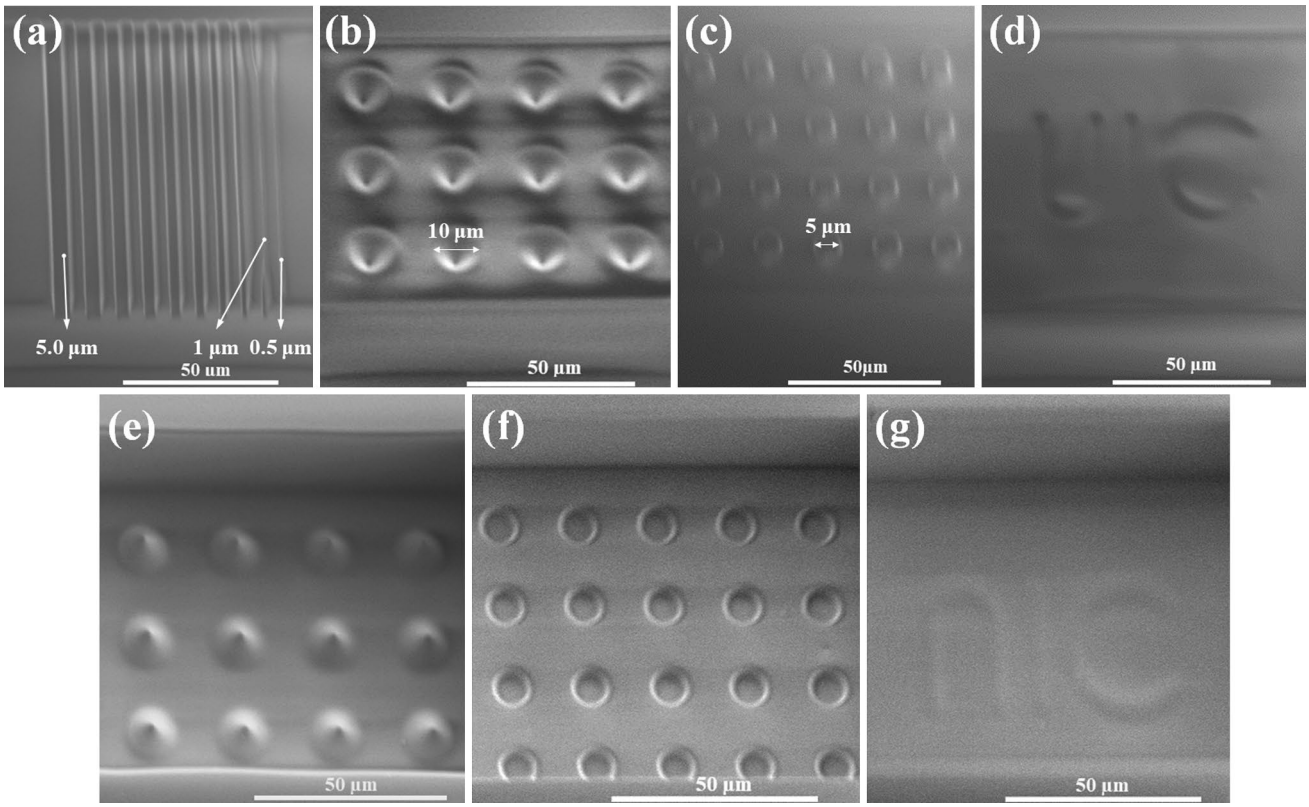

Fig. 7 **a** SEM image of the block with various grooves ranging from 0.5 to 5.0 µm. **b–d** SEM images of various designs fabricated via hybrid method, including cone-shaped cavities, cylindrical pillars, and UIC characters, respectively. **e–g** SEM images of corresponding PDMS replicas, respectively

Table 1 Time cost for three different designs (40 µm thick) using hybrid method or pure TPP

Structures	Prebake (min)	Exposure	Quick postbake	TPP process	Postbake (min)	Development (min)
Connecting block with cone-shape cavities	10	45 s	20 s	14 min 53 s	8	5
Connecting block with cylindrical pillars	10	45 s	20 s	10 min 55 s	8	5
Connecting block with UIC characters	10	45 s	20 s	15 min 53 s	8	5
Pure TPP for main channel (solid)	10	N/A	N/A	928 h 20 min	8	5
Pure TPP for main channel (scaffold)	10	N/A	N/A	131 h 18 min	8	5

main channel of micromixer was fabricated using photolithography while three gaps were later filled with three chaotic mixing components using TPP. As presented in Fig. 8a, b, each chaotic mixing component composed of four triangular blocks that were organized alternatively. Pillars with the diameter of 6 µm and length of 12 µm were also added to the surfaces of the blocks to further agitate the flows. After creating the PDMS-based device using as-fabricated mould, we injected the solution of 0.02% w/v fluorescein sodium salt (Sigma-Aldrich) and DI water into two inlets at the flow rate of 0.5 ml/min, respectively (Fig. 8c). It is worth noting that after two chaotic mixing components, they were mixed completely.

4 Conclusion

To summarize, we have successfully developed a new method to create master moulds for soft lithography using the combination of photolithography and TPP. It not only takes the advantages of traditional photolithography, where relatively large structures can be simply and rapidly

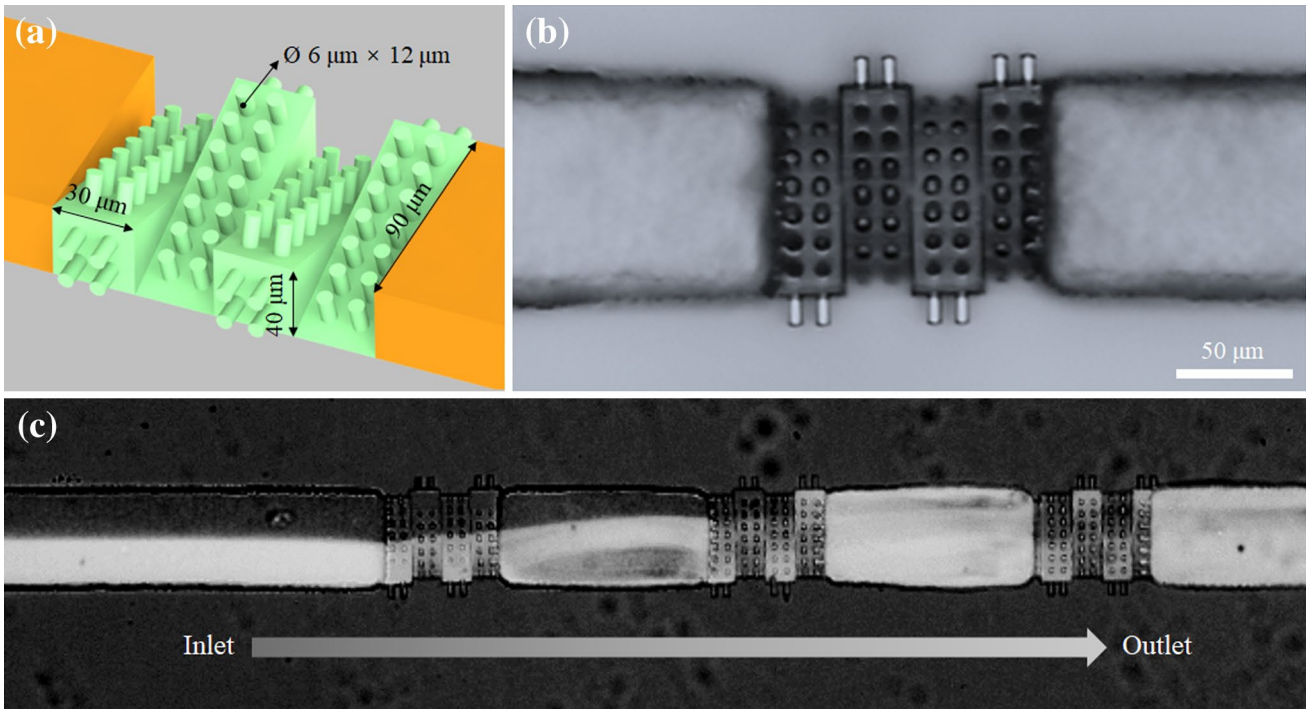

Fig. 8 A passive mixer fabricated using hybrid fabrication method. **a** Schematic illustration of the mixing component composed of four triangular blocks. **b** Image of the mixing component in a fabricated soft lithography master mould. **c** Image that showed a complete mixing achieved after two mixing components

fabricated, but also incorporates 3D fabrication using TPP. Hereby, the proposed method avoids the huge time expenses that are inevitable when creating the entire structures by TPP. Additionally, various complex 3D structures can be created in the region of interest with high resolution. Moreover, owing to the advantages of soft lithography, even though the master mould should be fabricated in a clean room, it can be used for multiple times to create PDMS replicas, further reducing the costs for single device.

Nevertheless, the hybrid method still has its own deficiencies. For instance, as the exact thickness of SU-8 film remains unknown before the TPP process, a careful prediction is required to minimize the difference in thicknesses between two structures. Additionally, as the alignment of TPP-based structures to existing exposed pattern is based on the clarity of exposed edges, the operational errors are inevitable. Thereby, the small shifts between two structures often exist. Besides, an addition of the second droplet of immersion oil on the top of SU-8 exerts additional stress on final structures, thus requiring a careful development process. An optimal laser intensity is also demanding to obtain reliable master moulds as well as avoiding bubble formation during the TPP process. Finally, the structures were fabricated on a brittle and thin glass cover slide, thus care should always be taken when handling the process. Nonetheless, this method has proposed a new approach to create complicated microfluidic devices with high resolution in a simple and faster way.

Acknowledgements This work was supported by an Early Career Faculty grant (80NSSC17K0522) from NASA's Space Technology Research Grants Program.

References

Baldacchini T (2015) Three-dimensional microfabrication using two-photon polymerization: fundamentals, technology, and applications. William Andrew, Norwich

Bernardeschi I, Tricinci O, Mattoli V, Filippeschi C, Mazzolai B, Beccai L (2016) Three-dimensional soft material micropatterning via direct laser lithography of flexible molds. ACS Appl Mater Interfaces 8:25019–25023

Borenstein JT, Tupper MM, Mack PJ, Weinberg EJ, Khalil AS, Hsiao J, García-Cardeña G (2010) Functional endothelialized microvascular networks with circular cross-sections in a tissue culture substrate. Biomed Microdevice 12:71–79

Brittman S, Oener SZ, Guo K, Āboliņš H, Koenderink AF, Garnett EC (2017) Controlling crystallization to imprint nanophotonic structures into halide perovskites using soft lithography. J Mater Chem C 5:8301–8307

Carugo D, Lee JY, Pora A, Browning RJ, Capretto L, Nastruzzi C, Stride E (2016) Facile and cost-effective production of microscale PDMS architectures using a combined micromilling-replica moulding (µMi-REM) technique. Biomed Microdevices 18:4

Childs WR, Nuzzo RG (2002) Decal transfer microlithography: a new soft-lithographic patterning method. J Am Chem Soc 124:13583–13596

Choi J-H, Lee S-K, Lim J-M, Yang S-M, Yi G-R (2010) Designed pneumatic valve actuators for controlled droplet breakup and generation. Lab Chip 10:456–461

del Campo A, Greiner C (2007) SU-8: a photoresist for high-aspect-ratio and 3D submicron lithography. J Micromech Microeng 17:R81

Filipponi L, Livingston P, Kašpar O, Tokárová V, Nicolau DV (2016) Protein patterning by microcontact printing using pyramidal PDMS. stamps. Biomed Microdevices 18:9

Folch A (2016) Introduction to bioMEMS. CRC Press, Boca Raton

Huang Y, Paloczi GT, Yariv A, Zhang C, Dalton LR (2004) Fabrication and replication of polymer integrated optical devices using electron-beam lithography and soft lithography. J Phys Chem B 108:8606–8613

Huh D, Matthews BD, Mammoto A, Montoya-Zavala M, Hsin HY, Ingber DE (2010) Reconstituting organ-level lung functions on a chip. Science 328:1662–1668

Hwang Y, Paydar OH, Candler RN (2015) 3D printed molds for non-planar PDMS microfluidic channels. Sens Actuators A Phys 226:137–142

Jeon NL, Hu J, Whitesides G, Erhardt MK, Nuzzo RG (1998) Fabrication of silicon MOSFETs using soft lithography. Adv Mater 10:1466–1469

Jiang LJ et al (2014) Two-photon polymerization: investigation of chemical and mechanical properties of resins using Raman microspectroscopy. Opt Lett 39:3034–3037

Kai Y (2004) Wafer warpage detection during bake process in photolithography

Kamei K-i et al (2015) 3D printing of soft lithography mold for rapid production of polydimethylsiloxane-based microfluidic devices for cell stimulation with concentration gradients. Biomed Microdevices 17:36

Kane RS, Takayama S, Ostuni E, Ingber DE, Whitesides GM (2006) Patterning proteins and cells using soft lithography. In: The biomaterials: Silver Jubilee compendium. Elsevier, Amsterdam, pp 161–174

Kim E, Xia Y, Whitesides GM (1995) Polymer microstructures formed by moulding. in capillaries. Nature 376:581

Kim P, Kwon KW, Park MC, Lee SH, Kim SM, Suh KY (2008) Soft lithography for microfluidics: a review

King E, Xia Y, Zhao XM, Whitesides GM (1997) Solvent-assisted microcontact molding: A convenient method for fabricating three-dimensional. structures on surfaces of polymers. Adva Mater 9:651–654

Kurihara M, Heo Y, Kuribayashi-Shigetomi K, Takeuchi S (2012) 3D laser lithography combined with Parylene coating for the rapid fabrication of 3D microstructures. In: Micro Electro Mechanical Systems (MEMS), 2012 IEEE 25th International Conference on IEEE, pp 196–199

Li H-W, Kang D-J, Blamire M, Huck WT (2003) Focused ion beam fabrication of silicon. print masters. Nanotechnology 14:220

Lin Y, Xu J (2018) Microstructures fabricated by two-photon polymerization and their remote manipulation techniques: toward 3D printing of micromachines. Adv Opt Mater 6:1701359

Lin C-H, Lee G-B, Chang B-W, Chang G-L (2002) A new fabrication process for ultra-thick microfluidic microstructures utilizing SU-8 photoresist. J Micromech Microeng 12:590

Mata A, Fleischman AJ, Roy S (2006) Fabrication of multi-layer SU-8 microstructures. J Micromech Microeng 16:276

Merkel T, Bondar V, Nagai K, Freeman B, Pinnau I (2000) Gas sorption, diffusion, and permeation in poly. (dimethylsiloxane). J Polym Sci Part B Polym Phys 38:415–434

Miyajima H, Mehregany M (1995) High-aspect-ratio photolithography for MEMS applications. J Microelectromech Syst 4:220–229

Narimannezhad A, Jennings J, Weber MH, Lynn KG (2013) Fabrication of high aspect ratio micro-Penning-Malmberg gold plated silicon trap arrays arXiv preprint arXiv:13072335

Pang M, Lin J, Cheng Z, Fu J, Xing R, Wang S (2003) Patterning and luminescent properties of nanocrystalline Y 2 O 3: Eu 3 + phosphor films by sol–gel soft lithography. Mater Sci Eng B 100:124–131

Park J, Li J, Han A (2010) Micro-macro hybrid soft-lithography master (MMHSM) fabrication for lab-on-a-chip applications. Biomed Microdevices 12:345–351

Qin D, Xia Y, Whitesides GM (2010) Soft lithography for micro-and nanoscale patterning. Nat Protoc 5:491–502

Rogers JA, Nuzzo RG (2005) Recent progress in soft lithography. Mater Today 8:50–56

Saive R, Bukowsky CR, Atwater HA (2017) Three-dimensional nanoimprint lithography using two-photon lithography master samples arXiv preprint arXiv:170204012

Schneider F, Draheim J, Kamberger R, Wallrabe U (2009) Process and material properties of polydimethylsiloxane (PDMS) for optical. MEMS Sens Actuators A Phys 151:95–99

Shin YS et al (2003) PDMS-based micro PCR chip with parylene coating. J Micromech Microeng 13:768

Sun Y, Zhang Z, Wong C (2005) Photo-definable nanocomposite for wafer level packaging. In: Electronic Components and Technology Conference Proceedings. 55th, 2005. IEEE, pp 179–184

Tan SH, Nguyen N-T, Chua YC, Kang TG (2010) Oxygen plasma treatment for reducing hydrophobicity of a sealed. polydimethylsiloxane microchannel. Biomicrofluidics 4:032204

Waldner J-B (2013) Nanocomputers and swarm intelligence. Wiley, Hoboken

Weiss I, Marom DM Direct 3D nano-printing on optical fiber tip. In: Optical MEMS and Nanophotonics (OMN), 2015 International Conference on (2015) IEEE, pp 1–2

Whitesides GM, Ostuni E, Takayama S, Jiang X, Ingber DE (2001) Soft lithography in biology and biochemistry. Annu Rev Biomed Eng 3:335–373

Xia Y, Whitesides GM (1998) Soft lithography. Ann Rev Mater Sci 28:153–184

Xu Q, Rioux RM, Dickey MD, Whitesides GM (2008) Nanoskiving: a new method to produce arrays of nanostructures. Acc Chem Res 41:1566–1577

Yang P et al (2000) Mirrorless lasing from mesostructured waveguides patterned by soft lithography. Science 287:465–467

Zhu B, Jin Y, Hu X, Zheng Q, Zhang S, Wang Q, Zhu J (2017) Poly (dimethylsiloxane) thin film as a stable interfacial layer for high-performance lithium-metal battery anodes. Adv Mater. https://doi.org/10.1002/adma.201603755